Strain broadening of the 1042-nm zero phonon line of the NV$^-$ center in diamond: A promising spectroscopic tool for defect tomography

T. B. Biktagirov,[1] A. N. Smirnov,[2] V. Yu. Davydov,[2] M. W. Doherty,[3] A. Alkauskas,[4,5] B. C. Gibson,[6] and V. A. Soltamov[1,2]

[1]*Kazan Federal University, Kazan 420008, Russia*

[2]*Ioffe Institute, St. Petersburg 194021, Russia*

[3]*Laser Physics Centre, Research School of Physics and Engineering, Australian National University, Australian Capital Territory 2601, Australia*

[4]*Center for Physical Sciences and Technology, Vilnius LT-10257, Lithuania*

[5]*Department of Physics, Kaunas University of Technology, Kaunas LT-51368, Lithuania*

[6]*ARC Centre of Excellence for Nanoscale BioPhotonics, School of Science, RMIT University, Melbourne, Victoria 3001, Australia*

(Received 20 January 2017; published 18 August 2017)

The negatively charged nitrogen-vacancy (NV$^-$) center in diamond is a promising candidate for many quantum applications. Here, we examine the splitting and broadening of the center's infrared (IR) zero-phonon line (ZPL). We develop a model for these effects that accounts for the strain induced by photodependent microscopic distributions of defects. We apply this model to interpret observed variations of the IR ZPL shape with temperature and photoexcitation conditions. We identify an anomalous temperature-dependent broadening mechanism and that defects other than the substitutional nitrogen center significantly contribute to strain broadening. The former conclusion suggests the presence of a strong Jahn-Teller effect in the center's singlet levels and the latter indicates that major sources of broadening are yet to be identified. These conclusions have important implications for the understanding of the center and the engineering of diamond quantum devices. Finally, we propose that, once the major sources of broadening are identified, the IR ZPL has the potential to be a sensitive spectroscopic tool for probing microscopic strain fields and performing defect tomography.

DOI: 10.1103/PhysRevB.96.075205

I. INTRODUCTION

In recent years, the negatively charged nitrogen-vacancy (NV$^-$) center in diamond has attracted numerous research efforts aimed toward a wide range of applications. This color center exhibits long ground-state spin coherence and optically induced spin polarization over a broad range of wavelengths in ambient conditions, which makes it a perfect candidate for quantum sensing applications [1–6], room-temperature-operated masers [7], and quantum computing [8–10].

The inhomogeneous broadening of the optical and spin resonances of NV$^-$ centers is a key limitation of many of these applications. It is currently believed that this inhomogeneous broadening is principally caused by the inhomogeneous strain and electromagnetic fields generated by random microscopic distributions of defects in the diamond, such as the substitutional nitrogen (N) center [11–13]. However, the correlation between microscopic defect density and inhomogeneous broadening has not yet been quantitatively studied, and so this hypothesis has not yet been rigorously tested. Better understanding of the sources of inhomogeneous broadening will ultimately support superior engineering of diamond quantum devices.

The NV$^-$ center manifests two zero-phonon lines (ZPL) [Fig. 1(a)], the visible 1.946 eV (637 nm) and infrared (IR) 1.190 eV (1042 nm) associated with triplet-triplet $^3A_2 \leftrightarrow {}^3E$ and singlet-singlet $^1E \leftrightarrow {}^1A_1$ transitions, respectively [14]. The $^1E \leftrightarrow {}^1A_1$ transition plays a crucial role in the spin dynamics of the NV$^-$ center because, along with the triplet-singlet nonradiative intersystem crossings (ISCs) [shown by the dashed arrows in Fig. 1(a)], it is part of the spin-dependent channel that enables the optical spin polarization and readout of the center's ground state spin [14]. Thus, further study of the IR ZPL is important to the understanding of the properties of the singlet levels and the ISCs [15,16].

In this paper, we report a detailed study of the splitting and inhomogeneous broadening of the NV$^-$ center's IR ZPL. We interestingly find that the splitting and broadening can be reduced by increasing excitation intensity or reducing excitation wavelength. To explain these observations, we develop a model for the inhomogeneous broadening that includes the strain induced by photodependent microscopic distributions of point defects. We use this model to distinguish strain broadening from other sources of broadening and, by doing so, identify an anomalous temperature-dependent broadening mechanism, which potentially provides additional evidence of a strong Jahn-Teller effect in the ^{1}E level. We show that the quantified strain broadening cannot be completely accounted for by the presence of N centers, thereby suggesting that there are major sources of broadening yet to be identified. We propose that the IR ZPL has the potential to be used as a sensitive spectroscopic tool to probe the microscopic distribution of strain fields and, with further work that identifies the major sources of strain, to perform tomography of defect concentrations.

II. EXPERIMENTAL METHOD

Two different diamond samples containing NV$^-$ centers were studied in this work. The main difference between the samples was the concentration of N centers. Sample 1 (S1) was a type IIa single crystal diamond plate with dimensions $3\times3\times0.3$ mm that was fabricated commercially by Element-6 using chemical-vapor deposition (CVD). The initial concentration of N was $\lesssim$100 ppb. The sample was

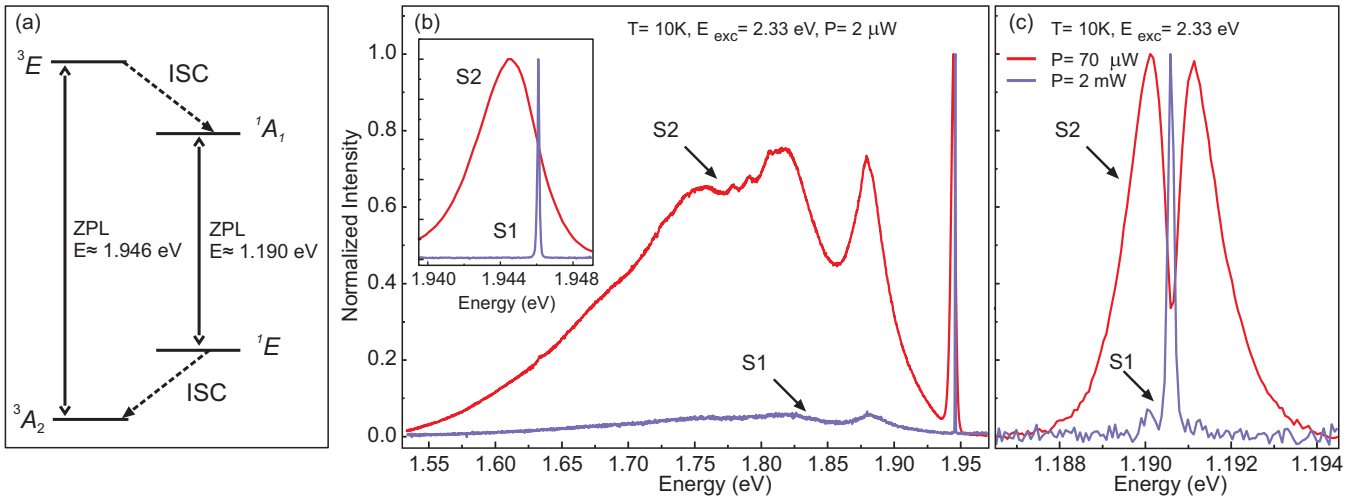

FIG. 1. (a) The NV^- center's electronic structure, including the low temperature visible E ≈1.946 eV and infrared E ≈1.190 eV ZPL energies indicated by the solid arrows, and the spin-dependent nonradiative intersystem crossings (ISCs) between the triplet and singlet levels. (b, c) PL spectra recorded at $T = 10$ K in samples S1 and S2 in the ranges of the NV^- center's visible and IR ZPLs, respectively. The energy (E_{exc}) and power (P) of the excitation laser are as indicated. The inset in (b) shows the visible ZPL with enlarged scale.

irradiated to a total dose of 10^{18} cm^{-2} with 900 keV electrons without control of the irradiation temperature. Sample 2 (S2) was a type Ib single crystal diamond plate with dimensions 3×3×0.3 mm that was fabricated commercially by Element-6 using high-pressure high-temperature (HPHT) growth and initially contained ≲200 ppm of N. The sample was irradiated with 3–5 MeV neutrons at temperatures close to room temperature to a total dose of 10^{18} cm^{-2}. S2 was then annealed at a temperature $T = 800\,^{\circ}C$ for 2 h in the presence of a forming gas (H2) in order to achieve a high density of NV^- centers via the capture of mobile vacancies by N centers [17,18]. S1 was not subjected to any thermal treatment, but may have undergone substantial heating to vacancy annealing temperature during irradiation. Thus, in summary, S1 has low densities of NV and N, whereas S2 has high densities.

The optical properties of the NV^- centers in each sample was studied by performing microphotoluminescence (PL) measurements using a Horiba Jobin-Yvon T64000 spectrometer equipped with a confocal microscope and a closed-cycle helium system for cryogenic microscopy. A Nd:YAG-laser line 2.33 eV (532 nm) and a He-Ne-laser line 1.96 eV (632.8 nm) were used for photoexcitation. The beam imaging, normal to the surface, was focused by a Mitutoyo 100xNIR (NA = 0.50) objective lens into each sample with a spot size of ∼2 μm. The same objective collected the PL. We used a CCD camera together with 1800 and 600 lines/mm gratings to measure the PL spectra with the spectral resolution of ≈0.05 meV in the visible and IR ranges, respectively.

III. RESULTS AND ANALYSIS

A. Comparison of the visible and IR zero-phonon lineshapes

We start with the comparison of the PL spectra of the NV^- centers in samples S1 and S2 that are presented in Figs. 1(b) and 1(c). At a glance, there are significant differences in both the visible and IR ZPLs of the samples. In S1, narrow ZPLs were observed with simple Gaussian inhomogeneous lineshapes characterized by full widths at half maximum (FWHM) of ∼0.14 meV (visible) and ∼0.2 meV (IR). In S2, the visible and IR ZPLs differ significantly. The visible ZPL in S2 has shifted and broadened relative to S1 [inset in Fig 1(b)], whereas the IR ZPL in S2 has instead split and broadened.

The differing inhomogeneous lineshapes of the visible and IR ZPLs in S2 can be qualitatively explained by recalling that the ZPLs have different susceptibilities [19,20] to inhomogeneous strain and electric fields induced by random distributions of defects [11–13]. Being a type Ib diamond, the most prevalent defect in S2 is expected to be the N center. In thermal equilibrium, the N center adopts a neutral charge state N^0. In this state, the center is paramagnetic and spontaneously undergoes a large distortion where one of the N-C bonds is substantially elongated [21]. The known stress susceptibility parameters of the visible and IR ZPLs [19] imply that the strain induced by a N^0 center's distortion will primarily shift the visible ZPL of a proximal NV^- center, while primarily splitting its IR ZPL. Averaging over the strain fields induced by many N^0 centers as well as over many NV^- sites, one therefore expects to observe an inhomogeneously broadened visible ZPL without a splitting and an inhomogeneously broadened IR ZPL with a discernible splitting, as exhibited in Figs. 1(b) and 1(c).

Now, under photoexcitation with photon energy ≳1.7 eV [22,23], the N^0 center can be photoionized to form the positive charge state N^+. In this state, the center is nonparamagnetic and returns to an undistorted configuration where the N atom resides at the substitutional site [24]. As a result, N^+ generates an electric field due to its charge but induces minimal strain. Since first-principles theory predicts that the IR ZPL is not susceptible to electric fields [25], the photoionization of N^0 to N^+ should lead to narrowing of the IR ZPL, thereby providing a means to test that N^0 is indeed the dominant source of inhomogeneous broadening. The same is not true for the visible ZPL because it is known to be susceptible to electric fields [14]. Therefore, any narrowing of the visible ZPL due to the smaller strain generated by N^+ will be countered by additional broadening due to the electric field it produces. Consequently,

in the following we focus on the IR ZPL as a tool to probe the sources of inhomogeneous broadening.

B. Model of the IR zero-phonon lineshape

To quantitatively describe the inhomogeneous broadening of the IR ZPL, we adapt the model of defect-induced strain broadening proposed in Refs. [26] and [27] for rare earth doped inorganic crystals. The key assumptions of the model are that the strain contributions from individual point defects are isotropic, add linearly and the crystal is well-approximated by an isotropic elastic continuum. In the model, the strain-induced changes of the two transition energies $\nu_{\pm}$ of the IR ZPL are

$$\nu_{\pm} = V(A_1)e(A_1) + V(A_1^{'})e_1(A^{'}) \pm \sqrt{V^2(E)[e_1(E)+e_2(E)]^2+V^2(E^{'})[e_1(E^{'})+e_2(E^{'})]^2}, \quad (1)$$

where $e(A_1) = e_{xx} + e_{yy} + e_{zz}$, $e(A_1^{'}) = \frac{1}{2}(2e_{zz} - e_{xx} - e_{yy})$, $e_1(E) = e_{yy} - e_{xx}$, $e_2(E) = 2e_{xy}$, $e_1(E^{'}) = 2e_{xz}$, and $e_2(E^{'}) = 2e_{yz}$ are the deformation tensor components that have been defined to have explicit C_{3v} symmetry properties in the coordinate frame of the NV center, and $V(A_1)$, $V(A_1^{'})$, $V(E)$, and $V(E^{'})$ are the corresponding strain susceptibility parameters of the IR ZPL. The susceptibility parameters can be obtained from those reported in terms of stress in the crystal coordinate system in Ref. [19] by applying the elastic constants of the crystal and performing the required coordinate frame rotations. One finds that $V(A_1) = 636.48$, $V(A_1^{'}) = -437.76$, $V(E) = -1567.17$, $V(E^{'}) = -1373.22$ in units of meV/strain for the IR ZPL. Note that from the above expression for $\nu_{\pm}$, it can be seen that the IR ZPL splits due to the deformations of E symmetry, while it shifts due to those of A_1 symmetry.

Following Ref. [27], assuming locally uniform densities of point defects, the statistical distribution function of the deformation tensor components $\mathbf{e} \equiv [e_1(E), e_2(E), e_1(E^{'}), e_2(E^{'})]$ is

$$g(\mathbf{e}) = \frac{3\gamma}{4\pi^2}[e_1(E)^2 + e_2(E)^2 + e_1(E^{'})^2 + e_2(E^{'})^2 + \gamma^2]^{-5/2}, \quad (2)$$

where the distribution width $\gamma = \frac{\pi}{27}\frac{1+\sigma}{1-\sigma}\{\sum_i [c[i]\Delta V[i]/V)^2\}^{1/2}$ depends on the Poisson ratio of diamond $\sigma = 0.2$ [28], the fractional concentration $c[i]$ of the ith species of point defect and the volume strain $\Delta V[i]/V$ per unit fractional concentration of defects of the ith species [26,27]. The strain broadened lineshape of the IR ZPL is then the convolution of $g(\mathbf{e})$ and a Gaussian lineshape

$$I(\nu) \propto \int d\mathbf{e} g(e)\left(\exp\left\{-\frac{[\nu-\nu_0-\nu_-]^2}{2\Delta^2}\right\} + \exp\left\{-\frac{[\nu-\nu_0-\nu_+]^2}{2\Delta^2}\right\}\right), \quad (3)$$

where the Gaussian width Δ accounts for the broadening induced by the deformations of A_1 symmetry, all other inhomogeneous broadening (not arising from strain induced by point defects) and homogeneous broadening. Notably, the defect-induced broadening parameter γ defines the splitting of the IR ZPL and contributes to its linewidth, whereas the Gaussian width Δ just contributes to the linewidth. In the above, the integration is taken over the four E symmetry deformation tensor components, and ν_0 is the energy of the unperturbed IR ZPL. This integration must be performed numerically. Note that we have not explicitly treated the broadening induced by the deformations of A_1 symmetry because, as supported by the following observations, the smaller strain shift of the IR ZPL implies that their contributions to the width Δ are negligible compared to the other sources of inhomogeneous and homogeneous broadening.

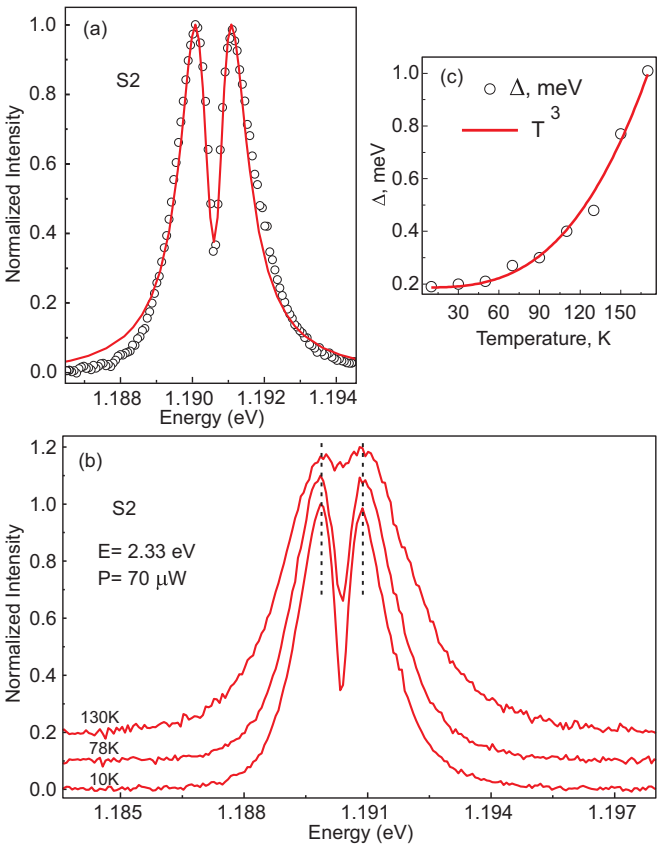

FIG. 2. (a) The fit (solid line) of the IR ZPL spectra (circles) of S2 from Fig. 1(c) using the inhomogeneous lineshape expression Eq. (3). The fit parameters are $\gamma = 1.7\times10^{-4}$ and $\Delta = 0.18$ meV. (b) Temperature dependence of the IR ZPL shape for S2. The dashed lines serve as a guide to demonstrate the temperature independence of the strain-induced splitting. The fixed photoexcitation energy and power are denoted in the figure. (c) Plot showing the temperature dependence of the fitted Gaussian width Δ. Experimental (circles) and fit (solid line) obtained using the power law $\Delta(T) = \Delta_0 + a\times T^3$. The fit parameters are $\Delta_0 = (0.18 \pm 0.1)$ meV and $a = 1.65\times10^{-4}$ meV K^{-3}.

C. Anomalous temperature-dependent broadening of the IR ZPL

As demonstrated in Fig. 2(a), our expression for $I(\nu)$ successfully describes the inhomogeneous lineshape of the IR ZPL in S2. Figure 2(b) depicts the temperature dependence of the IR ZPL under the same photoexcitation conditions. The dashed lines in Fig. 2(b) indicate that the ZPL splitting

does not change with temperature, thereby implying that the strain induced broadening is temperature independent. The temperature dependence of the ZPL rather arises from the $\propto T^3$ temperature variation of the Gaussian width Δ that is plotted in Fig. 2(c). Such temperature-dependent broadening has been observed in the NV^- center's visible ZPL [29] and the ZPLs of other defects in diamond [30] and attributed to temperature-dependent electron-phonon scattering. This is likely to be the case also for the IR ZPL; however, it must be noted that some caution must be exercised because the Gaussian width Δ is not purely related to the homogeneous broadening that would arise from electron-phonon scattering but also has contributions from other mechanisms of inhomogeneous broadening. If this complication is ignored, then our results suggest that the electron-phonon scattering affecting the IR ZPL has a somewhat unusual $\propto T^3$ temperature variation. Although a similar temperature variation has been observed for the ZPL of the negatively charged silicon-vacancy (SiV^-) center, this has been shown to be a modification of the usual $\propto T^5$ Raman-type scattering mechanism by the large spin-orbit interaction of the SiV^- center [30]. No such spin-orbit interaction can be present in the singlet levels involved in the NV^- center's IR ZPL. It is possible that the $\propto T^3$ temperature variation of the IR ZPL arises from the presence of a strong Jahn-Teller effect [31], which is consistent with the dramatic asymmetry of photoabsorption and PL spectra of the IR ZPL's vibrational sideband that is currently poorly understood [32]. However, substantial further investigation is required before this conclusion can be drawn.

D. Nitrogen-induced broadening of the IR ZPL

To test the role of N^0 in strain broadening, we analyzed the dependence of the IR ZPL on the photoexcitation energy and power. As can be seen in Fig. 3(a), increasing the photoexcitation energy (decreasing wavelength) with fixed power and temperature results in the decrease of γ with almost constant Δ. A result that is consistent over the two different positions in S2 that we sampled. Figure 3(b) demonstrates that increasing the photoexcitation power with fixed energy and temperature similarly results in the decrease of γ with almost constant Δ. These results support the hypothesis described above that increased photoionization of N^0 at higher photoexcitation energies and powers will reduce strain broadening. This hypothesis is further supported by the fit of the photoexcitation power dependence of γ in Fig. 3(c) by a simple two-state rate equation model of N^0 photoionization. Defining a power-dependent photoionization rate BP and a power independent recombination rate A, the steady-state concentration of N^0 is

$$c[\mathrm{N}^0](P) = c[\mathrm{N}^0](0)\frac{1}{1+\Omega P}, \tag{4}$$

where $c[N^0](0)$ is the concentration of N^0 at zero power and $\Omega = B/A$. The steady-state expression for γ is then

$$\gamma(P) = \left\{\gamma[\mathrm{other}]^2 + \left[\gamma[\mathrm{N}^0](0)\frac{1}{1+\Omega P}\right]^2\right\}^{1/2}, \tag{5}$$

where $\gamma[\mathrm{N}^0](0) = \frac{\pi}{27}\frac{1+\sigma}{1-\sigma}c[\mathrm{N}^0](0)\frac{\Delta V[\mathrm{N}^0]}{V}$ is the strain broadening due to N^0 at zero power and γ[other] is the power-independent strain broadening due to all other sources. The parameter values obtained from the fit in Fig. 3(c) are $\gamma[\mathrm{other}] = 1.30 \pm 0.04$, $\gamma[\mathrm{N}^0](0) = 1.27 \pm 0.07$, and $\Omega = 0.004 \pm 0.002\ \mu\mathrm{W}^{-1}$.

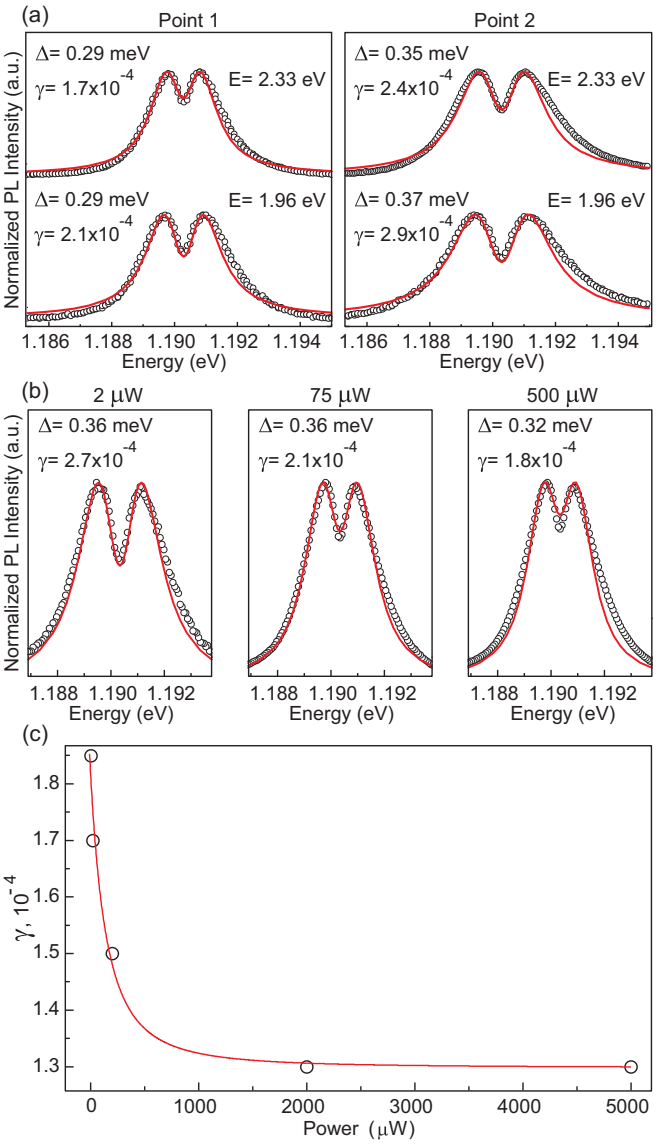

FIG. 3. Experimental (circles) and simulated (solid lines) IR ZPL spectra (a) for different excitation energies (2.33 and 1.96 eV) at two points of S2 taken at the laser power P = 70 μW, and (b) for different powers of the 2.33 eV excitation laser. (c) the power dependence of the extracted value of γ (points) from spectra at a third point in S2 with 2.33 eV excitation. The solid line denotes the fit described in the text. All spectra were recorded at temperature $T = 78$ K.

The power dependence of the strain broadening $\gamma(P)$ appears to imply the unexpected conclusion that N^0 causes at most $\gamma[\mathrm{N}^0](0)/\{\gamma[\mathrm{other}] + \gamma[\mathrm{N}^0](0)\} \approx 50\%$ of the strain broadening, thereby indicating that major sources of strain broadening are yet to be identified. The other defects known to be in the sample are NV^-, its neutral charge state NV^0, and the vacancy (V) center. The concentrations of NV and NV^0 must be less than N^0 by growth arguments and our annealing of S2 is expected to almost completely remove V centers. It is possible

that divacancy centers formed during annealing [33]. Although these should be lower in concentration than N and NV centers since the concentration of available vacancies generated by the neutron irradiation (accounting for annihilation by interstitials during annealing) is expected to be less than the initial N concentration. Owing to their much lower concentrations, for these centers (NV, V, and divacancy) to be the major sources of strain broadening, they must induce much larger strains than N^0, which is unlikely due to their comparable atomic size to N^0. We dismiss the possibility of multi-nitrogen related complexes (e.g., H3 and N3 centers) being present in appreciable concentrations because S2 is a type Ib diamond, implying nitrogen is primarily present as an isolated substitutional, and the annealing temperature following irradiation was too low for the nitrogen to migrate to form complexes [34].

Another issue arises in the quantitative analysis of the fit parameters. Using the value of $\Delta V[N^0]/V = 0.41$ that has been obtained from x-ray crystallography [35], the fitted value of $\gamma[N^0](0)$ yields a N^0 concentration of $c[N^0](0) \approx 1775$ ppm at zero photoexcitation power, which is $\sim$10 times larger than the specification of $\lesssim$200 ppm that was assigned by the sample supplier. Possible origins of this overestimation are incorrect specification by the supplier, large nonuniformity of N^0 concentration over the sample or photoionization of NV^-. Considering the latter further, it is known that NV^- photoionizes to NV^0 under excitation with energy >1.946 eV [14]. Thus, photoionization of NV^- could occur under the excitation conditions we employed. However, similar to before, for photoionization of NV^- to explain the overestimation, the difference in strain induced by NV^- and NV^0 must be much larger than the difference between N^0 and N^+.

E. *Ab initio* modeling of defect-induced broadening

To test these explanations, we have performed density functional theory (DFT) calculations of the strain induced by N^0, N^+, NV^-, and NV^0 centers. Calculations were performed using the VASP program [36] and employed the screened hybrid functional of Heyd, Scuseria, and Ernzerhof HSE06 to describe the electronic structure [37]. Interaction between ions and valence electrons were treated with the PAW approach [36]. Wave functions were expanded in plane waves (using 400 eV for the kinetic energy cutoff). We have used 216 (512) atom supercells to model N^0 and N^+ (NV^- and NV^0). The Brillouin zone was sampled at the Γ point to make sure local symmetry is properly represented. Defect-induced stress was calculated as the average of the three diagonal stress components $p = (\sigma_{xx} + \sigma_{yy} + \sigma_{yy})/3$ in the supercell, mimicking the averaging over different defect orientations. Subsequently, p was corrected for a small residual stress of the pristine supercell when calculated using exactly the same computational parameters (k-point sampling, cutoff energy, and the supercell size). Crucially, stress of charged defects (N^+ and NV^-) has been corrected for the spurious potential alignment term contribution using the procedure of Bruneval *et al.* (Eq. (26) in the Ref. [38]). Absolute deformation potentials of bulk diamond states needed for that procedure have been taken from calculations reported in Ref. [39]. Finally, volume expansion coefficient has been determined via $V[i]/V = p/(Bx)$, where $B = 481$ GPa is the calculated bulk modulus of diamond (cf. the experimental value of 443 GPa), and x is the concentration of defects in our supercells (either $1/216$ or $1/512$).

TABLE I. The volume strain per unit concentration of various defects in diamond as we have calculated using DFT and as obtained previously [35] by experiment.

$V[i]/V$	N^0	N^+	NV^-	NV^0
Calc.	0.23	0.01	−0.16	0.00
Expt.	0.41	—	—	—

The results of our DFT calculations are summarized in Table I. The value for the volume strain ($V[N^0]/V$) per unit fractional concentration of N^0 underestimates the experimental value by $\sim$50%. Part of this disagreement stems from the shortcomings of DFT and, likely, relatively large defect concentrations in actual calculations. However, the disagreement can also arise from experimental errors in determining the actual nitrogen concentration. In agreement with expectations, the value for N^+ is negligible. The value for NV^- is negative, which is consistent with the expectations based upon the presence of a vacancy in the defect. Interestingly, the value of $V[i]/V$ for NV^0 is almost zero, which reflects a small outward relaxation of atoms adjacent to the vacancy in NV^0 as compared to NV^-. Importantly, the magnitudes of the values for N^0 and NV^- are comparable, and thus, in accordance with the arguments above, we can conclude that NV^- is not the unidentified major source of broadening nor is its photoionization the explanation for the overestimation of the N^0 concentration. The resolution of these issues requires further investigation beyond this work. Such future work should include the confirmation of the average concentration of N^0 in the samples using electron paramagnetic resonance and infrared absorption spectroscopy as well as the systematic study of large nonuniformities of the N^0 concentration in the samples. Indeed, evidence of the latter can be immediately seen in the variation of γ between the two positions in S2 that are depicted in Fig 3. If the issues can be resolved, then analysis of the strain broadening of the NV^- center's IR ZPL will be a promising tool for defect micro-/nanoscale tomography.

IV. CONCLUSION

To summarize, we have reported a detailed study of the splitting and inhomogeneous broadening of the NV^- center's IR ZPL. We have identified that its inhomogeneous lineshape differs from the center's visible ZPL because the IR ZPL has a different susceptibility to strain fields and is not susceptible to electric fields. This singular susceptibility motivated the use of the IR ZPL to quantify the broadening due to different microscopic distributions of defects via the strain fields that they generate. We developed a model of the inhomogeneous lineshape of the IR ZPL by adapting the strain broadening theory proposed in Refs. [26] and [27]. We applied the model to interpret observations of temperature variation of the IR ZPL shape. By distinguishing strain broadening from other sources of broadening, we identified an anomalous $\propto T^3$ temperature-dependent broadening mechanism, which potentially provides

additional evidence of a strong Jahn-Teller effect in the ^{1}E level. This additional evidence furthers the understanding the singlet levels of the NV^- center and their role in the center's optical spin polarization and readout mechanisms.

We interestingly found that the strain broadening of the IR ZPL can be reduced by increasing excitation intensity or reducing excitation wavelength. Through the application of our model, these effects were found to be qualitatively consistent with the photodependence of the concentration of N^0 centers. However, quantitative analysis revealed that only ≈50% of the strain broadening can be attributed to the photodependence of N^0, thereby indicating that there exist other, yet to be identified, sources of strain broadening. Furthermore, the quantitative analysis yielded an estimate of the local N^0 concentration that was ∼10 times larger than what the supplier specified as the average concentration. To investigate these issues further, we performed DFT calculations of the strain induced by different charge states of N and NV centers. These calculations supported our initial interpretation and thus did not resolve these issues of the quantitative analysis. We conclude that further work is required to identify the unidentified sources of broadening and to test the estimation of the local concentration of N^0. Given this further work, we proposed that the IR ZPL has the potential to be used as a sensitive spectroscopic tool to probe the microscopic distribution of strain fields and to perform tomography of defect concentrations.

ACKNOWLEDGMENTS

This work has been supported by the ARC Grants No. FT110100225, No. CE140100003, and No. DE170102735, and performed according to the Russian Government Program of Competitive Growth of Kazan Federal University. B.C.G. acknowledges the support of the ARC Centre of Excellence for Nanoscale BioPhotonics (CNBP) and an ARC Future Fellowship. V.A.S. acknowledges the support of the RFBR Project No. 16-52-76017 (ERA.Net RUS Plus Project DIABASE). A.A. acknowledges the support of the Research Council of Lithuania via Grant No. M-ERA.NET-1/2015. Computations were performed at the High Performance Computing Center "HPC Sauletekis" in Faculty of Physics, Vilnius University. We acknowledge fruitful discussions with Boris Malkin, Sergey Feofilov, and Neil Manson.

[1] G. R. Balasubramanian, P. Neumann, D. Twitchen, M. Markham, R. Kolesov, N. Mizuochi, J. Isoya, J. Achard, J. Beck, J. Tissler, V. Jacques, P. R. Hemmer, F. Jelezko, and J. Wrachtrup, Ultralong spin coherence time in isotopically engineered diamond, Nat. Mater. **8**, 383 (2009).

[2] K. Arai, C. Belthangady, H. Zhang, N. Bar-Gill, S. J. DeVience, P. Cappellaro, A. Yacoby, and R. L. Walsworth, Fourier magnetic imaging with nanoscale resolution and compressed sensing speed-up using electronic spins in diamond, Nat. Nanotechnol. **10**, 859 (2015).

[3] F. Dolde, H. Fedder, M. W. Doherty, T. Nbauer, F. Rempp, G. Balasubramanian, T. Wolf, F. Reinhard, L. C. L. Hollenberg, F. Jelezko, and J. Wrachtrup, Electric-field sensing using single diamond spins, Nat. Phys. **7**, 459 (2011).

[4] G. Kucsko, P. C. Maurer, N. Y. Yao, M. Kubo, H. J. Noh, P. K. Lo, H. Park, and M. D. Lukin, Nanometre-scale thermometry in a living cell, Nature **500**, 54 (2013).

[5] M. W. Doherty, V. V. Struzhkin, D. A. Simpson, L. P. McGuinness, Y. Meng, A. Stacey, T. J. Karle, R. J. Hemley, N. B. Manson, L. C. L. Hollenberg, and S. Prawer, Electronic Properties and Metrology Applications of the Diamond NV^- Center Under Pressure, Phys. Rev. Lett. **112**, 047601 (2014).

[6] D. R. Glenn, K. Lee, H. Park, R. Weissleder, A. Yacoby, M. D. Lukin, H. Lee, R. L. Walsworth, and C. B. Connolly, Single-cell magnetic imaging using a quantum diamond microscope, Nat. Methods **12**, 736 (2015).

[7] L. Jin, M. Pfender, N. Aslam, P. Neumann, S. Yang, J. Wrachtrup, and R.-B. Liu, Proposal for a room-temperature diamond maser, Nat. Commun. **6**, 8251 (2015).

[8] G. Waldherr, Y. Wang, S. Zaiser, M. Jamali, T. Schulte-Herbrueggen, H. Abe, T. Ohshima, J. Isoya, J. F. Du, P. Neumann, and J. Wrachtrup, Quantum error correction in a solid-state hybrid spin register, Nature **506**, 204 (2014).

[9] N. Y. Yao, L. Jiang, A. V. Gorshkov, P. C. Maurer, G. Giedke, J. I. Cirac, and M. D. Lukin, Scalable architecture for a room temperature solid-state quantum information processor, Nat. Commun. **3**, 800 (2012).

[10] B. Hensen, H. Bernien, A. E. Drau, A. Reiserer, N. Kalb, M. S. Blok, J. Ruitenberg, R. F. L. Vermeulen, R. N. Schouten, C. Abellán, W. Amaya, V. Pruneri, M. W. Mitchell, M. Markham, D. J. Twitchen, D. Elkouss, S. Wehner, T. H. Taminiau, and R. Hanson, Loophole-free Bell inequality violation using electron spins separated by 1.3 kilometres, Nature **526**, 682 (2015).

[11] A. M. Stoneham, Shapes of inhomogenously broadened resonance lines in solids, Rev. Mod. Phys. **41**, 82 (1969).

[12] G. Davies, No phonon lineshape and crystal strain fields in diamonds, J. Phys. C: Solid State Phys. **3**, 2474 (1970).

[13] G. Davies, Approximate widths of zero phonon lines broadened by point defect strain fields, J. Phys. D: Appl. Phys. **4**, 1340 (1971).

[14] M. W. Doherty, N. B. Manson, P. Delaney, F. Jelezko, J. Wrachtrup, and L. C. L. Hollenberg, The nitrogen-vacancy color center in diamond, Phys. Rep. **528**, 1 (2013).

[15] M. L. Goldman, A. Sipahigil, M. W. Doherty, N. Y. Yao, S. D. Bennett, M. Markham, D. J. Twitchen, N. B. Manson, A. Kubanek, and M. D. Lukin, Phonon-Induced Population Dynamics and Intersystem Crossing in Nitrogen-Vacancy Centers, Phys. Rev. Lett. **114**, 145502 (2015).

[16] M. L. Goldman, M. W. Doherty, A. Sipahigil, N. Y. Yao, S. D. Bennett, N. B. Manson, A. Kubanek, and M. D. Lukin, State-selective intersystem crossing in nitrogen-vacancy centers, Phys. Rev. B **91**, 165201 (2015).

[17] Y. Mita, Change of absorption spectra in type-Ib diamond with heavy neutron irradiation, Phys. Rev. B **53**, 11360 (1996).

[18] V. M. Acosta, E. Bauch, M. P. Ledbetter, C. Santori, K.-M. C. Fu, P. E. Barclay, R. G. Beausoleil, H. Linget, J. F. Roch, F. Treussart, S. Chemerisov, W. Gawlik, and D. Budker, Diamonds with

a high density of nitrogen-vacancy centers for magnetometry applications, Phys. Rev. B **80**, 115202 (2009).

[19] L. J. Rogers, M. W. Doherty, M. S. J. Barson, S. Onoda, T. Ohshima, and N. B. Manson, Singlet levels of the NV^- center in diamond, New J. Phys. **17**, 013048 (2015).

[20] M. W. Doherty, N. B. Manson, P. Delaney, and L. C. L. Hollenberg, The negatively charged nitrogen-vacancy center in diamond: the electronic solution, New J. Phys. **13**, 025019 (2011).

[21] J. H. N. Loubser and J. A. van Wyk, Electron spin resonance in the study of diamond, Rep. Prog. Phys. **41**, 1201 (1978).

[22] R. G. Farrer, On the substitutional nitrogen donor in diamond, Solid State Commun. **7**, 685 (1969).

[23] J. Isberg, A. Tajani, and D. J. Twitchen, Photoionization measurement of deep defects in single-crystalline CVD diamond using the transient-current technique, Phys. Rev. B **73**, 245207 (2006).

[24] A. M. Stoneham, Theoretical status of diamond and its defects, excited states and atomic motion, Mater. Sci. Eng. B **11**, 211 (1992).

[25] Group theoretical arguments imply that to lowest-order in the electronic model of the NV center, the IR ZPL is not susceptible to strain or electric fields (electric and strain fields having identical symmetry properties) [20]. However, owing to the displacement of the centers electronic orbitals accompanying strain, the IR ZPL is susceptible to strain through the modification of the electronic repulsion energy [19]. An electric field will not result in such displacement. Thus, the IR ZPL is expected to be susceptible to strain but not electric fields.

[26] S. A. Klimin, D. S. Pytalev, M. N. Popova, B. Z. Malkin, M. V. Vanyunin, and S. L. Korableva, High-resolution optical spectroscopy of Tm^{3+} ions in LiYF4: Crystal-field energies, hyperfine and deformation splittings, and the isotopic structure, Phys. Rev. B **81**, 045113 (2010).

[27] B. Z. Malkin, D. S. Pytalev, M. N. Popova, E. I. Baibekov, M. L. Falin, K. I. Gerasimov, and N. M. Khaidukov, Random lattice deformations in rare-earth-doped cubic hexafluoroelpasolites: High-resolution optical spectroscopy and theoretical studies, Phys. Rev. B **86**, 134110 (2012).

[28] J. E. Field, The mechanical and strength properties of diamond, Rep. Prog. Phys. **75**, 126505 (2012).

[29] K.-M. C. Fu, C. Santori, P. E. Barclay, L. J. Rogers, N. B. Manson, and R. G. Beausoleil, Observation of the Dynamic Jahn-Teller Effect in the Excited States of Nitrogen-Vacancy Centers in Diamond, Phys. Rev. Lett. **103**, 256404 (2009).

[30] K. D. Jahnke, A. Sipahigil, J. M. Binder, M. W. Doherty, M. Metsch, L. J. Rogers, N. B. Manson, M. D. Lukin, and F. Jelezko, Electronphonon processes of the silicon-vacancy center in diamond, New J. Phys. **17**, 043011 (2015).

[31] V. Hizhnyakov, V. Boltrushko, H. Kaasik, and I. Sildos, Phase relaxation in the vicinity of the dynamic instability: Anomalous temperature dependence of zero-phonon line, J. Lumin. **107**, 351 (2004).

[32] P. Kehayias, M. W. Doherty, D. English, R. Fischer, A. Jarmola, K. Jensen, N. Leefer, P. Hemmer, N. B. Manson, and D. Budker, Infrared absorption band and vibronic structure of the nitrogen-vacancy center in diamond, Phys. Rev. B **88**, 165202 (2013).

[33] D. J. Twitchen, M. E. Newton, J. M. Baker, T. R. Anthony, and W. F. Banholzer, Electron-paramagnetic-resonance measurements on the divacancy defect center R4/W6 in diamond, Phys. Rev. B **59**, 12900 (1999).

[34] A. M. Zaitsev, *Optical Properties of Diamond: A Data Handbook* (Springer-Verlag, Berlin, 2010).

[35] A. R. Lang, M. Moore, A. P. W. Makepeave, W. Wierzchowski, and C. M. Welbourn, On the dilation of synthetic type Ib diamond by substitutional nitrogen impurity, Phil. Trans. R. Soc. London A **337**, 497 (1991).

[36] G. Kresse and J. Furthmüller, Efficient iterative schemes for *ab initio* total-energy calculations using a plane-wave basis set, Phys. Rev. B **54**, 11169 (1996); G. Kresse and D. Joubert, From ultrasoft pseudopotentials to the projector augmented-wave method, *ibid.* **59**, 1758 (1999).

[37] J. Heyd, G. E. Scuseria, and M. Ernzerhof, Hybrid functionals based on a screened Coulomb potential, J. Chem. Phys. **118**, 8207 (2003).

[38] F. Bruneval, C. Varvenne, J.-P. Crocombette, and E. Clouet, Pressure, relaxation volume, and elastic interactions in charged simulation cells, Phys. Rev. B **91**, 024107 (2015).

[39] Y.-H. Li, X. G. Gong, and S.-H. Wei, *Ab initio* all-electron calculation of absolute volume deformation potentials of IV-IV, III-V, and II-VI semiconductors: The chemical trends, Phys. Rev. B **73**, 245206 (2006).